Photodissociation Dynamics of Various Conformers of Iodobutane Isomer Ions Prepared Selectively by Vacuum Ultraviolet Mass-Analyzed Threshold Ionization

Sang Tae Park and Myung Soo Kim*

Contribution from the National Creative Research Initiative for Control of Reaction Dynamics and School of Chemistry, Seoul National University, Seoul 151-742, Korea

Received February 2, 2002

Abstract: Various conformers of $1\text{-}C_4H_9I^{+\bullet}$, $2\text{-}C_4H_9I^{+\bullet}$, and $i\text{-}C_4H_9I^{+\bullet}$ were prepared selectively by mass-analyzed threshold ionization with coherent vacuum ultraviolet radiation. Conformer-selective photodissociation of these ions was studied in the 560−730 nm spectral region, which corresponds to excitation to the first excited electronic state. Rapid dissociation was observed as manifested by noticeable laser polarization dependence of the product signals. In particular, photodissociation of $i\text{-}C_4H_9I^{+\bullet}$ was found to be conformer specific, occurring without interconversion between conformers. The product's asymptote energies estimated from the experimental data were compared with the reaction enthalpies at 0 K to get information on the structures and states of products. It was found that a simple S_N2-type mechanism deduced from the previous study of $1\text{-}C_3H_7I^{+\bullet}$ was compatible with the present observations. Validity of the widely adopted postulate in stereochemistry that different conformations can be gateways to different reactions has been demonstrated in the gas phase.

Introduction

Zero electron kinetic energy (ZEKE)[1] spectroscopy has been widely used to determine the ionization energies of neutrals and to obtain spectroscopic information on ions generated. Mass-analyzed threshold ionization (MATI)[2] is a technique based on the same principle, which detects ions instead of electrons in ZEKE. Even though spectroscopic resolution of MATI is not as good as ZEKE at the moment, it can be a useful technique to prepare state-selected polyatomic ions, especially near the ground vibronic states, for dynamics study.

Recently, we reported spectroscopic studies on iodopropane[3] and iodobutane[4] isomers with MATI using coherent vacuum ultraviolet (VUV) radiation generated by four-wave mixing in Kr gas. An important achievement in those works was the selective generation of various conformer ions from these molecules by tuning the VUV wavelength. In particular, conformer ions in the vibrationless ground electronic state could be generated selectively, which did not have sufficient internal energy to overcome the conformational barriers. Since collision-induced interchange between conformations would not occur either under the very high vacuum condition of the experiment, an ion beam of a particular conformation could be generated.

The capability of conformer-selective ionization was utilized in the subsequent work[5,6] to study conformation dependence of photodissociation of 1-iodopropane ion, $1\text{-}C_3H_7I^{+\bullet}$, which has two stable conformations in the ground state, gauche and anti. When $1\text{-}C_3H_7I^{+\bullet}$ was excited to the first excited electronic state,[5] it was found to dissociate rapidly in this state while further excited ions[6] were observed to undergo internal conversion to the ground state followed by dissociation. The most remarkable observation in the study was that dissociation in the first excited state, which has n ← σ (C−I) character, was conformer-specific, the gauche conformer ion generating $2\text{-}C_3H_7^+ + I\ (^2P_{1/2})$ and the anti form $cyclic\text{-}C_3H_7^+ + I\ (^2P_{1/2})$. Reaction path calculation at the single excitation configuration interaction (CIS)[7] level showed that dissociation of both conformers proceeded via the intramolecular S_N2 mechanism, the H or CH_3 moiety at the anti position with respect to iodine moving toward C(1). Also, observation of the conformer specificity was proof that $1\text{-}C_3H_7I^{+\bullet}$ generated in the ground vibronic state by VUV-MATI retained its conformation until excited by the photodissociation laser.

In this paper, we report the results from similar photodissociation studies on iodobutane isomers which display a wider variety of conformations. The main impetus for the present study was to see if the dissociation mechanism in the first excited electronic state of $1\text{-}C_3H_7I^{+\bullet}$ that rendered the conformer specificity, namely the intramolecular S_N2-type reaction, would be applicable also to other iodoalkane ions. Elucidating the role

---

* To whom correspondence should be addressed. Phone: +82-2-880-6652. Fax: +82-2-889-1568. E-mail: myungsoo@plaza.snu.ac.kr.

(1) (a) Schlag, E. W. *ZEKE Spectroscopy*; Cambridge University Press: Cambridge, UK, 1998. (b) Müller-Dethlefs, K.; Schlag, E. W. *Annu. Rev. Phys. Chem.* **1991**, *42*, 109−136.

(2) (a) Zhu, L.; Johnson, P. *J. Chem. Phys.* **1991**, *94*, 5769−5771. (b) Krause, H.; Neusser, H. J. *J. Chem. Phys.* **1992**, *97*, 5923−5926.

(3) Park, S. T.; Kim, S. K.; Kim, M. S. *J. Chem. Phys.* **2001**, *114*, 5568−5576.

(4) Park, S. T.; Kim, S. K.; Kim, M. S. *J. Chem. Phys.* **2001**, *115*, 2492−2498.

(5) Park, S. T.; Kim, S. K.; Kim, M. S. *Nature* **2002**, *415*, 306−308.

(6) Park, S. T.; Kim, M. S. *J. Chem. Phys.* In press.

(7) Foresman, J. B.; Head-Gordon, M.; Pople, J. A.; Frisch, M. J. *J. Phys. Chem.* **1992**, *96*, 135−149.

of conformations of these ions in the production of various butyl ions was the secondary focus of this work.
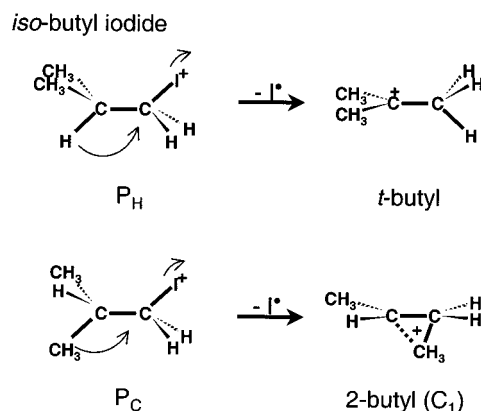
Experimental Section

Iodobutanes were purchased from Aldrich and used without further purification. The samples kept at room temperature were seeded in helium or argon carrier gas and expanded into a source vacuum chamber through a 0.5 mm diameter nozzle orifice (General Valve). The supersonic jet was then skimmed through a 1 mm diameter skimmer (Beam Dynamics) to enter a differentially pumped ionization chamber. The backing pressure was typically 1−3 atm and the background pressure of the ionization chamber was maintained below 10^{-7} Torr.

Since details of the experimental setup and method were described previously,[3−6] only a brief outline will be provided here. Coherent VUV radiation in the 134−136 nm region was generated by four-wave mixing[8] in a Kr cell with the pressure optimized in the 1−10 Torr range. Two laser pulses were used for this purpose, one at 212.4 nm and the other at 480−520 nm. The VUV laser pulse thus generated was collinearly overlapped with the molecular beam in a counter-propagation manner[9] to excite neutral molecules to Rydberg states close to the ionization limit. A short scrambling field pulse[10] was applied at the time of VUV laser irradiation. A spoil field of ∼0.5 V/cm was applied to separate directly generated ions from the highly excited neutrals. The latter were ionized by a 125 V/cm pulse applied ∼20 μs after the VUV pulse. For photodissociation, another laser output in the 560−730 nm region was irradiated perpendicular to both the molecular beam and ion flight directions ∼100 ns after pulsed-field ionization. Rochon polarizer/half-wave plate combinations were used to change the polarization angle of the photodissociation laser with respect to the ion flight direction. Time-of-flight (TOF) mass spectrometry was used to record the parent and fragment ion signals.

Results and Discussion

A series of bands appear in the photoelectron spectra of iodobutane isomers.[11] Ionization to the spin−orbit doublet of the ground electronic state, $\tilde{X}_1$ and $\tilde{X}_2$, was the focus of our previous MATI study of these molecules.[4] Peak tops of the first excited electronic states, $\tilde{A}$, appear at 2.05, 1.95, 2.02, and 1.78 eV above the $\tilde{X}_1$ state in the photoelectron spectra of 1-iodobutane, 2-iodobutane, isobutyl iodide, and *tert*-butyl iodide, respectively. All these bands appear diffuse indicating ultrashort lifetimes of the $\tilde{A}$ states. In the present work, various conformer ions of iodobutane isomers in the vibrationless $\tilde{X}_1$ states have been generated selectively by adjusting the VUV wavelength and then irradiated with laser in the 560−730 nm region to study dissociation in the $\tilde{A}$ states. For t-C$_4$H$_9$I$^{+\bullet}$, photodissociation signal was not detectable possibly due to the very small transition probability compared to others. Photodissociation of t-C$_4$H$_9$I$^{+\bullet}$ is not of much interest in this work because it possesses only one stable conformation. In the other cases, C$_4$H$_9$$^+$ was the only fragment ion generated by photodissociation in the above spectral region.

The TOF profiles of C$_4$H$_9$$^+$ were found to be broadened due to the release of kinetic energy in the center-of-mass coordinate

(8) (a) Hilber, G.; Lago, A.; Wallenstein, R. *J. Opt. Soc. Am. B* **1987**, *4*, 1753−1764. (b) Marangos, J. P.; Shen, N.; Ma, H.; Hutchinson, M. H. R.; Conerade, J. P. *J. Opt. Soc. Am. B* **1990**, *7*, 1254−1259.
(9) Nir, E.; Hunziker, H. E.; De Vries, M. S. *Anal. Chem.* **1999**, *71*, 1674−1678.
(10) (a) Held, A.; Aigner, U.; Baranov, L. Y.; Selzle, H. L.; Schlag, E. W. *Chem. Phys. Lett.* **1999**, *299*, 110−114. (b) Held, A.; Baranov, L. Y.; Selzle, H. L.; Schlag, E. W. *Chem. Phys. Lett.* **1998**, *291*, 318−324. (c) Held, A.; Selzle, H. L.; Schlag, E. W. *J. Phys. Chem.* **1996**, *100*, 15314−15319.
(11) Kimura, K.; Katsumata, S.; Achiba, Y.; Yamazaki, T.; Iwata, S. *Handbook of HeI Photoelectron Spectra of Fundamental Organic Molecules*; Japan Scientific Societies: Tokyo, Japan, 1981.

Figure 1. P$_H$ and P$_C$ conformers of i-C$_4$H$_9$I$^{+\bullet}$ and their dissociation via intramolecular S$_N$2 reaction.

system and the fragment angular distribution. The latter is given by[12,13]

$$I(\Theta) = (1/4\pi)[1 + \beta P_2(\cos \Theta)] \tag{1}$$

Here Θ is the angle between the laser polarization and fragment recoil directions and P_2 denotes the second-order Legendre polynomial. β is the anisotropy parameter that is affected by the type of transition and by the rapidity of recoil compared to molecular rotation. It was reported previously[6,14] that the distributions of kinetic energy release and anisotropy can be obtained by analyzing the profiles recorded at several polarization angles. Even though the TOF profiles were taken at the laser polarization angles of 0°, 35.3°, 54.7°, and 90° with respect to the ion flight direction and analyzed satisfactorily, only the profiles at 0° and 90° will be shown for simplicity.
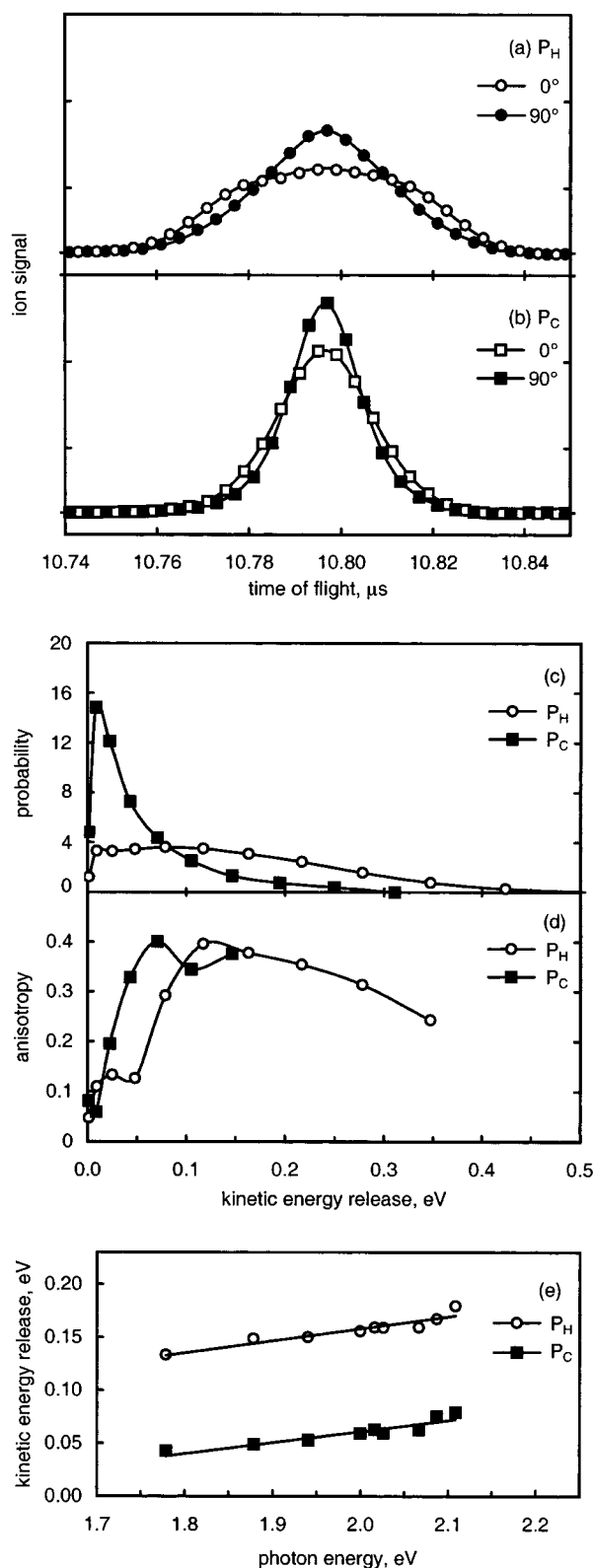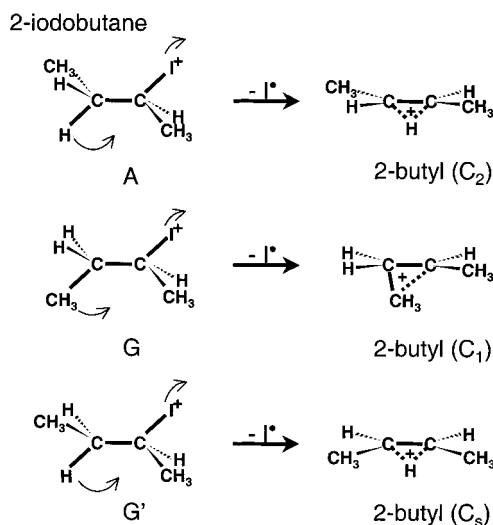
A. Isobutyl Iodide. i-C$_4$H$_9$I$^{+\bullet}$ has two stable conformations, P$_H$ and P$_C$ forms as shown in Figure 1, which were clearly resolved in the previous MATI spectrum.[4] The molecular ions of these conformers in the vibrationless ground state were selectively generated by MATI in this work with VUV wavelengths of 135.17 and 134.81 nm for P$_H$ and P$_C$ conformers, respectively. Figure 2a,b shows the TOF profiles of C$_4$H$_9$$^+$ generated by photodissociation of P$_H$ and P$_C$ conformers, respectively, at 615 nm with the polarization of the photodissociation laser parallel (0°) or perpendicular (90°) to the ion flight direction. It is to be noted that the fragment TOF profiles from the two conformers are noticeably different, the profile of P$_H$ being broader regardless of the laser polarization. This means that the kinetic energy release (KER, T) in the photodissociation of this conformer is larger than that for P$_C$. Also to be noted in the figure is the significant polarization dependence of the two profiles. This is due to rapid recoil of the fragments compared to molecular rotation. Distributions of KER and β determined from these profiles are shown in Figure 2, panels c and d, respectively. The average KERs, $\langle T \rangle$, evaluated from the distributions are 0.158 ± 0.013 and 0.063 ± 0.006 eV for P$_H$ and P$_C$ conformers, respectively, while the average anisotropies, $\langle \beta \rangle$, are 0.31 ± 0.05 and 0.24 ± 0.03. We repeated the measurement at various wavelengths of the photodissociation laser in the visible region. $\langle T \rangle$ vs the photon energy, or the

(12) Busch, G. E.; Wilson, K. R. *J. Chem. Phys.* **1972**, *56*, 3638−3654.
(13) Zare, R. N. *Mol. Photochem.* **1972**, *4*, 1−37.
(14) Kim, D. Y.; Choe, J. C.; Kim, M. S. *J. Chem. Phys.* **2000**, *113*, 1714−1724.
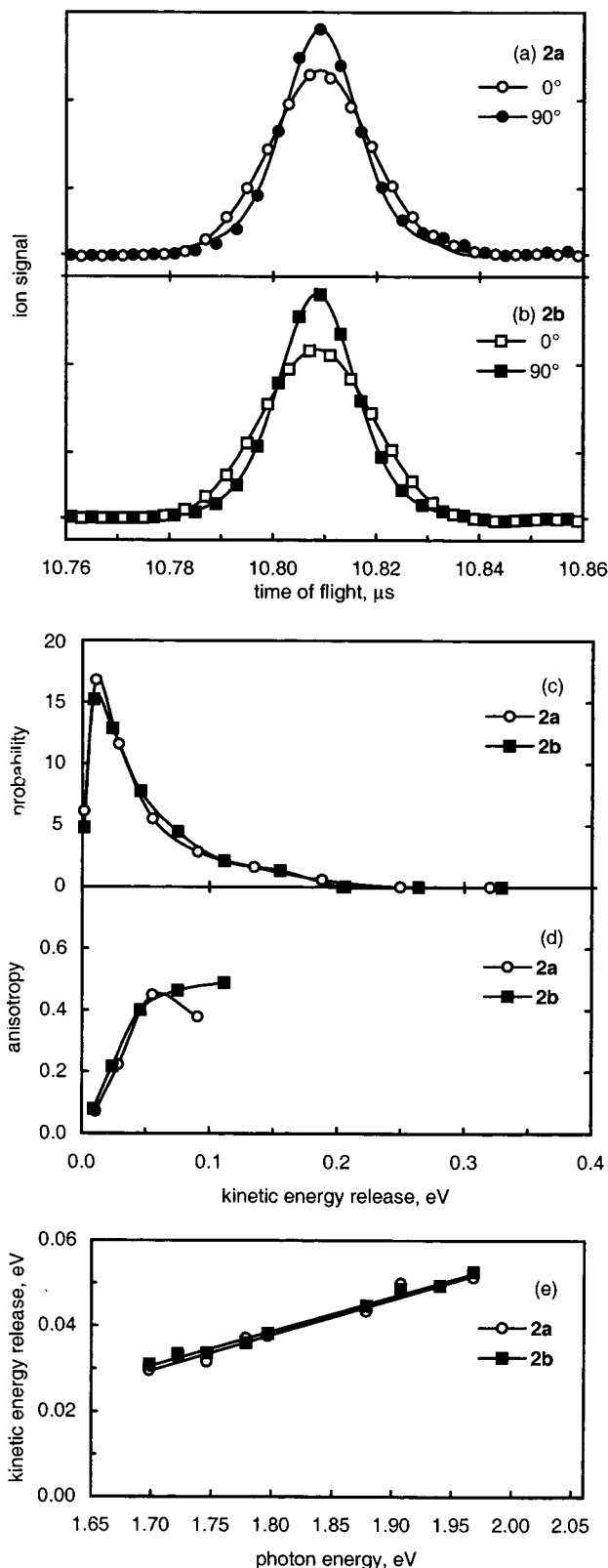
Figure 3. A, G, and G′ conformers of 2-$C_4H_9I^{+\bullet}$ and their dissociation via intramolecular S_N2 reaction.

internal energy of the photoexcited i-$C_4H_9I^{+\bullet}$ referred to the zero-point level in the ground electronic state, obtained from these measurements is shown in Figure 2e. For both conformers, $\langle T \rangle$ vs internal energy plots look linear just as found in the previous study on 1-$C_3H_7I^{+\bullet}$.[5] The threshold energies for dissociation of i-$C_4H_9I^{+\bullet}$, namely the product ($C_4H_9^+$ + I$^\bullet$) asymptote energy referred to the zero-point level in the ground electronic state of i-$C_4H_9I^{+\bullet}$, have been determined by linear extrapolation as was done for 1-$C_3H_7I^{+\bullet}$.[5] These were 0.61 ± 0.33 and 1.41 ± 0.21 eV respectively for P_H and P_C conformers. It should be mentioned that the P_H and P_C conformers of i-$C_4H_9I^{+\bullet}$ are analogous to the gauche and anti conformers of 1-$C_3H_7I^{+\bullet}$, respectively, in the sense that H and CH_3 moieties are located at the anti position with respect to the I atom. Then, the observation that the P_H conformer displays larger kinetic energy release and lower dissociation threshold than the P_C form parallels the observation made for 1-$C_3H_7I^{+\bullet}$. Detailed discussion on the dissociation mechanism and thermochemistry will be presented later.

B. 2-Iodobutane. Even though 2-$C_4H_9I^{+\bullet}$ can have three conformers, A, G, and G′ in Figure 3, only two conformers were detected in the previous MATI study.[4] These were probably A and G forms because the G′ form is the least stable of the three in the neutral. Conformer identification was not possible in the previous study, however. In the present study, the molecular ions of these conformers in the vibrationless ground states were produced by MATI at the VUV wavelengths of 136.42 and 136.38 nm. Conformer ions generated at these wavelengths will be designated as **2a** and **2b**, respectively. The TOF profiles of $C_4H_9^+$ generated by photodissociation of **2a** and **2b** at 639 nm with the parallel and perpendicular polarizations of the photodissociation laser are shown in Figure 4, panels a and b, respectively. It should be noted that the TOF profiles from **2a** and **2b** are very similar, both in width and anisotropy. Distributions of KER and β obtained from these profiles are shown in Figure 4, panels c and d, respectively. $\langle T \rangle$ evaluated from the distributions are 0.049 ± 0.011 and 0.049 ± 0.009 eV for **2a** and **2b**, respectively, while $\langle \beta \rangle$ are 0.24 ± 0.10 and 0.27 ± 0.06 eV. $\langle T \rangle$ vs internal energy plot obtained by performing the measurements at various photodissociation wavelengths in the visible region is shown in Figure 4e. The

Figure 2. TOF profiles of $C_4H_9^+$ generated by photodissociation of (a) P_H and (b) P_C conformers of i-$C_4H_9I^{+\bullet}$ at 615 nm. Open and filled symbols represent profiles obtained with 0° and 90° polarizations of the photodissociation laser with respect to the time-of-flight axis, respectively. TOF profiles recalculated with the distributions of T and β obtained below are shown as lines. Distributions of (c) T and (d) β obtained by analyzing the TOF profiles. (e) Plots of $\langle T \rangle$ vs photon energy for the photodissociations for P_H and P_C conformers of i-$C_4H_9I^{+\bullet}$ to $C_4H_9^+$ + I$^\bullet$ in the visible region. The results for the P_H and P_C conformers are shown as the open circles and filled squares, respectively.
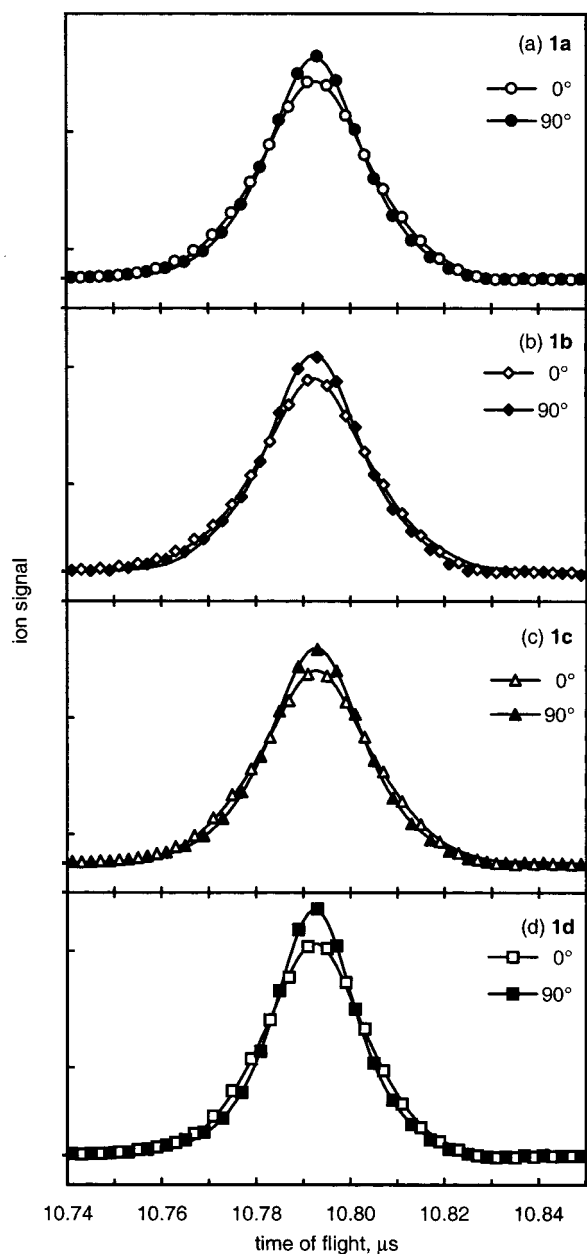
Figure 4. TOF profiles of $C_4H_9^+$ generated by photodissociation of (a) **2a** and (b) **2b** conformers of 2-$C_4H_9I^{+\bullet}$ at 639 nm. Open and filled symbols represent profiles obtained with 0° and 90° polarizations of the photodissociation laser with respect to the time-of-flight axis, respectively. TOF profiles recalculated with the distributions of T and β obtained below are shown as lines. Distributions of (c) T and (d) β obtained by analyzing the TOF profiles. (e) Plots of $\langle T \rangle$ vs photon energy for the photodissociations of 2-$C_4H_9I^{+\bullet}$ conformers to $C_4H_9^+ + I^\bullet$ in the visible region. The results for the **2a** and **2b** conformers are shown as the open circles and filled squares, respectively.
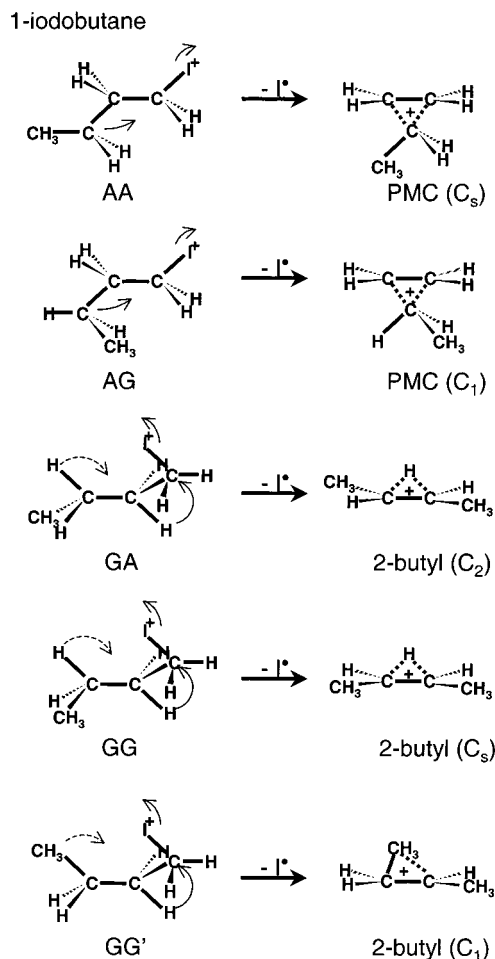
Figure 5. AA, AG, GA, GG, and GG′ conformers of 1-$C_4H_9I^{+\bullet}$ and their dissociation via intramolecular S_N2 reaction.

plots for **2a** and **2b** look almost identical. The dissociation thresholds estimated by linear extrapolation, 1.32 and 1.34 eV for **2a** and **2b**, respectively, were indistinguishable.
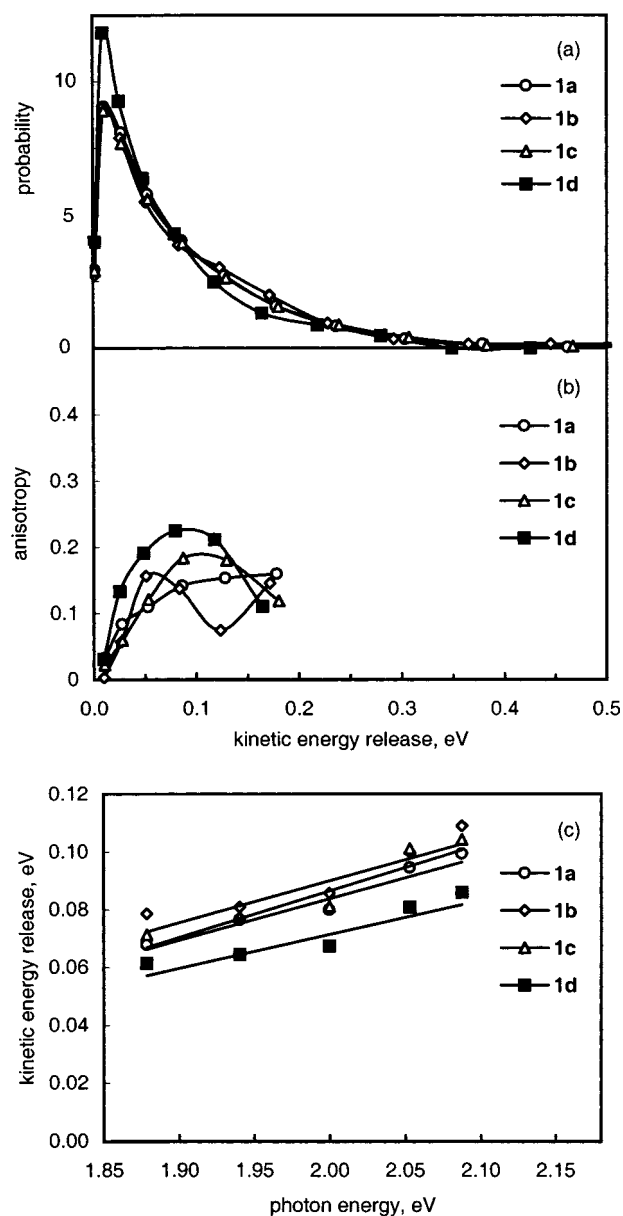
C. 1-Iodobutane. Only four out of five possible conformers, AA, AG, GA, GG, and GG′ (see Figure 5), of 1-$C_4H_9I^{+\bullet}$ were detected in the previous MATI study.[4] Conformer identification was not possible. In the present work, the molecular ions of these conformers in the vibrationless ground states were produced by MATI at the VUV wavelengths of 134.65, 134.59, 134.48, and 134.40 nm. Conformer ions generated at these wavelengths will be designated as **1a**, **1b**, **1c**, and **1d**, respectively. The TOF profiles of $C_4H_9^+$ generated by photodissociation of these conformer ions at 604 nm are shown in Figure 6. It should be noted that the TOF profiles from the four conformer ions look similar, in both width and anisotropy. Distributions of KER and β obtained from these profiles are shown in Figure 7, panels a and b, respectively. Distribution of KER from **1d** looks a little narrower and its average a little smaller than others. $\langle T \rangle$ vs internal energy plots obtained from photodissociation experiments at several wavelengths are shown in Figure 7c. It is to be noted that the plots from **1a**, **1b**, and **1c** conformers are virtually indistinguishable. The plot from **1d** conformer is close to the others. However, it shows consistently smaller $\langle T \rangle$ even though the experimental conditions were identical for all the cases except for the VUV wavelength used for MATI. The reaction thresholds estimated by linear extrapo-

Figure 6. TOF profiles of $C_4H_9^+$ generated by photodissociation of (a) **1a**, (b) **1b**, (c) **1c**, and (d) **1d** conformers of 1-$C_4H_9I^{+\bullet}$ at 605 nm. Open and filled symbols represent profiles obtained with 0° and 90° polarizations of the photodissociation laser with respect to the time-of-flight axis, respectively. TOF profiles recalculated with the distributions of T and β in Figure 7 (a and b) are shown as lines.

Figure 7. Distributions of (a) T and (b) β obtained by analyzing the TOF profiles of 1-$C_4H_9I^{+\bullet}$ conformers in Figure 6. (c) Plots of $\langle T \rangle$ vs photon energy for the photodissociations of 1-$C_4H_9I^{+\bullet}$ conformers to $C_4H_9^+$ + I$^\bullet$ in the visible region. The results for the **1a**, **1b**, **1c**, and **1d** conformers are shown as the open circles (○), diamond (◇), triangle (△), and filled squares (■), respectively.

lation are 1.42, 1.38, 1.46, and 1.39 eV for **1a**, **1b**, **1c**, and **1d**, respectively. From the threshold energy data alone, it may look as if **1b** and **1d** generate thermodynamically similar products. Considering the errors involved in experiments and data treatment, however, we would rather say that all four conformers generate thermodynamically similar products or that the products from **1d** are different from the others based on the consistently smaller KER.

D. Thermochemistry and Dissociation Mechanism. In our previous study on 1-$C_3H_7I^{+\bullet}$,[5] the dissociation thresholds estimated from the experimental data were compared with the enthalpies of reaction at 0 K for possible product channels. It was found that dissociation of the gauche conformer in the first excited electronic state generated 2-$C_3H_7^+$ + I ($^2P_{1/2}$) and the

anti form *cyclic*-$C_3H_7^+$ + I ($^2P_{1/2}$). Reaction path calculation at the CIS level supported the above conclusion and further showed that both of the conformers dissociate via an intramolecular S_N2-type process. The situation is much more complicated in the present case because of the presence of a variety of isomers and conformers of $C_4H_9I^{+\bullet}$ and $C_4H_9^+$ and hence pinpointing the mechanism of each reaction looks rather hopeless. Instead, we will just attempt to show that a thermochemically feasible channel for a particular reaction is also acceptable from the mechanistic point of view or can be explained by the intramolecular S_N2-type mechanism. It is to be kept in mind that the dissociation threshold was determined from the KER data in this work and hence is related to the structure of $C_4H_9^+$ at the time of C–I bond breaking. This structure can be different from the one determined by conventional mass spectrometric methods

Table 1. The Dissociation Thresholds for the Photodissociation of $C_4H_9I^{+\bullet} \rightarrow C_4H_9^+ + I^{\bullet}$, in eV

reactant	conformer	ΔE^a
i-$C_4H_9I^+$	P_H	0.61 ± 0.33
	P_C	1.41 ± 0.21
2-$C_4H_9I^+$	**2a**	1.32 ± 0.24
	2b	1.34 ± 0.25
1-$C_4H_9I^+$	**1a**	1.42 ± 0.18
	1b	1.38 ± 0.21
	1c	1.46 ± 0.18
	1d	1.39 ± 0.23

^{a} Product asymptote energy referred to the zero-point level of the reactant in the ground electronic state estimated as the x intercept in the linear extrapolation of $\langle T \rangle$ vs photon energy data.

Table 2. Enthalpy of Formation at 0 K Data Relevant to $C_4H_9I^{+\bullet} \rightarrow C_4H_9^+ + I^{\bullet}$, in eV

system		ΔH^0 (0 K)	ref
i-C_4H_9I		-0.32 ± 0.06^a	18
2-C_4H_9I		-0.35 ± 0.06^a	18
1-C_4H_9I		-0.23 ± 0.06^a	18
i-$C_4H_9I^+$	P_H	8.851 ± 0.06^b	4
	P_C	8.876 ± 0.06^b	4
2-$C_4H_9I^+$	**2a**	8.736 ± 0.06^b	4
	2b	8.739 ± 0.06^b	4
1-$C_4H_9I^+$	**1a**	8.980 ± 0.06^b	4
	1b	8.984 ± 0.06^b	4
	1c	8.991 ± 0.06^b	4
	1d	8.997 ± 0.06^b	4
t-$C_4H_9^+$	C_s	7.610^c	21
	C_{3h}	7.604 ± 0.034	4
	C_{3v}	7.660^c	21
2-$C_4H_9^+$	C_1	8.210^c	21
	C_2	8.191^c	21
	C_s	8.230^c	21
PMC	C_1	8.565^c	21
I ($^2P_{3/2}$)		1.1107	15
I ($^2P_{1/2}$)		2.0534	15

^{a} Taken from ref 18, which was estimated by group additivity methods. ^{b} Evaluated with ΔH_f^0 of neutral precursors in this table and conformer-specific ionization energies in ref 4. ^{c} Evaluated with use of data in ref 21. Experimental ΔH_f^0 for t-$C_4H_9^+$ in ref 4 was taken as the reference.

such as collision-induced dissociation and ion cyclotron resonance mass spectrometry. This is because the present method gets information on an incipient structure while the latter obtain structural information quite a long time after ion formation such that further isomerization may have changed the ionic structure. Also to be noted is that none of the KER distributions obtained in this work (see Figures 2c, 4c, and 7a) appear as a superposition of two or more components, indicating that each photo-excited conformer follows only one of many possible reaction paths. The thresholds for various dissociation reactions estimated in this work are listed in Table 1.

To compare with the experimental dissociation thresholds, one needs enthalpies of reaction at 0 K which, in turn, require the data of enthalpies of formation at 0 K, $\Delta H_f^0{}_{0K}$, for various structures and states of reactants and products. Relevant data to be described below are listed in Table 2. For the iodine atom, the states energetically accessible in the present work are the two components of the ground-state spin–orbit doublet, $^2P_{3/2}$ and $^2P_{1/2}$, for which $\Delta H_f^0{}_{0K}$ values are accurately known.[15] Also accurately known are the ionization energies of various isomers and conformers of C_4H_9I, which were determined in our previous MATI study.[4] To calculate $\Delta H_f^0{}_{0K}$ for various $C_4H_9I^{+\bullet}$ structures with the ionization energy data, one needs $\Delta H_f^0{}_{0K}$ data for the corresponding neutrals. $\Delta H_f^0{}_{298K}$ was experimentally

determined for t-C_4H_9I only,[16] which was converted to the 0 K value by Keister and co-workers.[17] Experimental data are not available for other isomers of C_4H_9I. Oliveira and co-workers[18] estimated these by the group additivity methods,[19] which were thought to be accurate within 6 kJ mol^{-1}. Among various $C_4H_9^+$ structures, t-$C_4H_9^+$ is known to be the most stable.[20–22] $\Delta H_f^0{}_{0K}$ of this ion was determined accurately, 733.7 ± 3.3 kJ mol^{-1}, in our previous MATI study,[4] which was in excellent agreement with 734 ± 3.6 kJ mol^{-1} reported by Keister et al.[17] 2-$C_4H_9^+$ is also known to be a stable species while 1-$C_4H_9^+$ and i-$C_4H_9^+$ are not stable species in the gas phase.[20,21] Since thermochemical data for $C_4H_9^+$ species are scarce, we utilized corresponding data obtained by Sieber and co-workers through high-level ab initio calculations.[21] t-$C_4H_9^+$, whose $\Delta H_f^0{}_{0K}$ is well established experimentally,[4,17] was used as the reference and $\Delta H_f^0{}_{0K}$ values for other species were estimated by taking into account the differences in the calculated values. Sieber and co-workers[21] identified three stable conformations of t-$C_4H_9^+$ with nearly the same energies. We took the C_{3h} form, which was reported to be the most stable after the zero-point energy correction, as the reference in this work. For 2-$C_4H_9^+$, classical open structures were reported to be unstable.[21] Instead, Sieber and co-workers identified three stable species with the C_1, H-bridged trans (C_2) and cis (C_s) forms. These structures are shown in Figure 3. $\Delta H_f^0{}_{0K}$ values of these structures are very similar (Table 2) and cannot be distinguished in the present work based on the dissociation threshold data. We also estimated $\Delta H_f^0{}_{0K}$ of this ion using $\Delta H_f^0{}_{0K}$(2-C_4H_9I), $\Delta H_f^0{}_{0K}$(I ($^2P_{3/2}$)), and the appearance energy of 2-$C_4H_9^+$ from 2-C_4H_9I measured in the previous MATI work. The 790 ± 6 kJ mol^{-1} (8.19 ± 0.06 eV) value thus obtained is in excellent agreement with values in Table 2 estimated from Sieber and co-workers' data. To compare with the experimental result, we converted the above to the 298 K value following the method in ref 23. 0 K data for C(s) and H_2 (g) in ref 15 were used. Also, vibrational frequencies of $C_4H_9^+$(g) obtained by ab initio calculation at the HF/6-31G* level were used (scale factor of 0.893). $\Delta H_f^0{}_{298K}$(2-$C_4H_9^+$) thus estimated was 764 ± 6 kJ mol^{-1}, in good agreement with the experimental value[22–24] of 766 ± 4 kJ mol^{-1}. Another important structure found by Sieber and co-workers[21] is the protonated methylcyclopropane (PMC) shown in Figure 5. Even though

(15) (a) Chase, M. W., Jr.; Davies, C. A.; Downey, J. R., Jr.; Frurip, D. J.; McDonald, R. A.; Syverud, A. N. JANAF Thermochemical Tables, 3rd. ed. *J. Phys. Chem. Ref. Data* **1985**, *14* (Suppl. 1). (b) Wagman, D. D.; Evans, W. H. E.; Parker, V. B.; Schum, R. H.; Halow, I.; Mailey, S. M.; Churney, K. L.; Nuttall, R. L. The NBS Tables of Chemical Thermodynamic Properties. *J. Phys. Chem. Ref. Data* **1982**, *11* (Suppl. 2). (c) Cox, J. D.; Wagman, D. D.; Medvedev, V. A. *CODATA Key Values for Thermodynamics*; Hemisphere: New York, 1989.
(16) Pedley, J. B.; Naylor, R. D.; Kirby, S. P. *Thermochemical Data of Organic Compounds*; Chapman and Hall: London, UK, 1986.
(17) Keister, J. W.; Riley, J. S.; Baer, T. *J. Am. Chem. Soc.* **1993**, *115*, 12613–12614.
(18) Oliveira, M. C.; Baer, T.; Olesik, S.; Ferreira, M. A. A. *Int. J. Mass Spectrom.* **1988**, *82*, 299–318.
(19) Benson, S. W. *Thermochemical Kinetics: Methods for the Estimation of Thermochemical Data and Rate Parameters*, 2nd ed.; Wiley-Interscience: New York, 1976.
(20) Vogel, P. *Carbocation Chemistry*; Elsevier: Amsterdam, The Netherlands, 1985.
(21) Sieber, S.; Buzek, P.; Schleyer, P. v. R.; Koch, W.; Carneiro, J. W. de M. *J. Am. Chem. Soc.* **1993**, *115*, 259–270.
(22) Aubry, C.; Holmes, J. L. *J. Phys. Chem. A* **1998**, *102*, 6441–6447.
(23) (a) Linstrom, P. J.; Mallard, W. G., Eds. *NIST Chemistry WebBook: NIST Standard Reference Database Number 69*; National Institute of Standards and Technology: Gaithersburg, MD, 2001 (http://webbook.nist.gov). (b) Lias, S. G.; Bartmess, J. E.; Liebman, J. F.; Holmes, J. L.; Levin, R. D.; Mallard, W. G. Gas-Phase Ion and Neutral Thermochemistry. *J. Phys. Chem. Ref. Data* **1988**, *17* (Suppl. 1).
(24) Traeger, J. C. *Org. Mass Spectrom.* **1981**, *16*, 193–194.

Table 3. Enthalpies of Reaction at 0 K Relevant to $C_4H_9I^{+\bullet} \rightarrow C_4H_9^+ + I^\bullet$, in eV[a]

	ΔH^0 (0 K)			
products	P_H	P_C	2a	1a
t-$C_4H_9^+$ + I ($^2P_{3/2}$)[b]	−0.136	−0.161	−0.021	−0.265
2-$C_4H_9^+$ + I ($^2P_{3/2}$)[c]	0.451	0.426	0.566	0.322
PMC + I ($^2P_{3/2}$)	0.824	0.799	0.939	0.695
t-$C_4H_9^+$ + I ($^2P_{1/2}$)[b]	0.806	0.782	0.922	0.678
2-$C_4H_9^+$ + I ($^2P_{1/2}$)[c]	1.394	1.369	1.509	1.265
PMC + I ($^2P_{1/2}$)	1.767	1.742	1.882	1.638

[a] Calculated with $\Delta H_f^0{}_{0K}$ data in Table 2. [b] $\Delta H_f^0{}_{0K}$ of t-$C_4H_9^+$ (C_{3h}) used. [c] $\Delta H_f^0{}_{0K}$ of 2-$C_4H_9^+$ (C_2) used.

protonated tetramethylene was also found to be a stable structure in the theoretical work,[21] this will not be considered in the present work as it is a high-energy species and also it is not generated from $C_4H_9I^{+\bullet}$ via the postulated mechanism.[5]

Using the $\Delta H_f^0{}_{0K}$ data in Table 2, we evaluated reaction enthalpies at 0 K for various possible dissociation channels. For i-$C_4H_9I^{+\bullet}$, both the P_H and P_C conformers were considered as the reactants because the dissociation thresholds measured for the two were significantly different. For 2-$C_4H_9I^{+\bullet}$, reaction enthalpy data evaluated for **2a** only will be presented for simplicity because **2a** and **2b** resulted in essentially identical data. Similarly, only **1a** was taken as the reactant for 1-$C_4H_9I^{+\bullet}$. Both $^2P_{3/2}$ and $^2P_{1/2}$ of the ground-state spin−orbit doublet were considered as possible states of the product iodine atom. For the fragment ion, t-$C_4H_9^+$, 2-$C_4H_9^+$ (C_2), and PMC were used for calculation. C_1 and C_s structures were not considered for 2-$C_4H_9^+$ because these are energetically identical with the C_2 form well within the accuracy of threshold determination in this work. The results are listed in Table 3.

The most feasible channel for each dissociation was determined by comparing the threshold data in Table 1 with the reaction enthalpy at 0 K data in Table 3. It was also assumed that the iodine atoms generated from different conformers of an isomer would be in the same spin−orbit state because the dissociation occurred in the same electronic state of the isomer, namely the first excited electronic state. For P_H and P_C conformers of i-$C_4H_9I^{+\bullet}$ (0.61 and 1.41 eV thresholds, respectively), it can be seen that 2-$C_4H_9^+$ + I ($^2P_{1/2}$) is the best candidate for the P_C conformer while the product assignment is ambiguous for the P_H form, candidates being 2-$C_4H_9^+$ + I ($^2P_{3/2}$), PMC + I ($^2P_{3/2}$), and t-$C_4H_9^+$ + I ($^2P_{1/2}$). With the assumption of the same spin−orbit state for the iodine atom produced from the P_H and P_C conformers, however, t-$C_4H_9^+$ + I ($^2P_{1/2}$) becomes the best candidate for the product channel for P_H. These assignments are in good agreement with the fragment ion structures expected from the intramolecular S_N2 mechanism postulated from the previous study[5] of 1-$C_3H_7I^{+\bullet}$, which results in t-$C_4H_9^+$ and 2-$C_4H_9^+$ (C_1), respectively, for dissociation of the P_H and P_C conformers (Figure 1). For 2-$C_4H_9I^{+\bullet}$, reaction thresholds measured for **2a** and **2b** forms are ~1.3 eV, which suggests generation of 2-$C_4H_9^+$ + I ($^2P_{1/2}$) according to the thermochemical data in Table 3. Figure 3 shows the intramolecular S_N2 processes for the A, G, and G′ conformers of 2-$C_4H_9I^{+\bullet}$ generating 2-$C_4H_9^+$ with C_2, C_1, and C_s structures that are energetically similar. Namely, the mechanistic interpretation is compatible with the observation that $\langle T \rangle$ vs internal energy plots for the **2a** and **2b** conformers are similar. Finally,

dissociation thresholds of 1.38−1.46 eV measured for **1a−d** conformers of 1-$C_4H_9I^{+\bullet}$ predict generation of 2-$C_4H_9^+$ or PMC or a mixture of both according to data in Table 3. Mechanistically, AA and AG conformers generate PMC (C_s) and PMC (C_1) as shown in Figure 5. Dissociation of GA, GG, and GG′ conformers cannot be explained by the one-step intramolecular S_N2 process because such a process results in the classical open structures of 2-$C_4H_9^+$ which were reported to be unstable. Concerted movement of a group (H or CH_3) from the C(3) position to C(2) results in the 2-$C_4H_9^+$ structures with C_1, C_2, and C_s symmetries as shown in Figure 5. Experimental $\langle T \rangle$ vs internal energy plots for the **1a−d** conformers were divided into two groups based on the actual magnitude of $\langle T \rangle$. According to the mechanistic analysis of the dissociation processes, it may well have arisen due to the generation of energetically distinct fragment ions, 2-$C_4H_9^+$ and PMC. However, experimental accuracy for the dissociation threshold is not sufficient enough to draw a firm conclusion on this aspect. The above investigation on 1-$C_4H_9I^{+\bullet}$ and 2-$C_4H_9I^{+\bullet}$ stopped short of identifying exact conformations of the reactants and products. However, it is to be noted that the experimental results clearly show that t-$C_4H_9^+$ is not the product in the photodissociation of these isomers. It is all the more meaningful because t-$C_4H_9^+$ is the most stable among the $C_4H_9^+$ isomers and is the statistically expected product. Hence, the present results can be taken as a demonstration of the role of conformation in determining the mechanistic pathway.

Summary and Conclusion

Even though the presence of various conformations of a molecule is frequently invoked to explain stereospecific aspects of a reaction,[25] direct investigation on the role of each conformation in the gas phase has been difficult. This is mainly because the barriers between conformations are usually very low such that interconversions between them are fast under ambient conditions.[26] In the present work, we have avoided the above difficulty by selectively preparing various conformers of $C_4H_9I^{+\bullet}$ by the VUV-MATI technique under very high vacuum conditions. Interconversion between conformers induced by activation needed for reaction has also been avoided by observing rapid dissociation occurring in the first excited electronic state. Analysis of the time-of-flight profiles of the fragments generated, $C_4H_9^+$, provided a useful dynamic fingerprint in the form of kinetic energy release. Even though the experimental data clearly showed that the dissociation process was affected by reactant conformation, definitive information on the detailed mechanism could not be drawn from these data because the structures of reactants and products were not known in most of the cases. Instead, we attempted to see if the propensity rules derived in our previous study[5,6] of 1-$C_3H_7I^{+\bullet}$ would be applicable in the present cases also. Namely, we estimated the reaction thresholds by linear approximation of the experimental data, as had been done for 1-$C_3H_7I^{+\bullet}$, determined the most plausible candidates for the products by comparing these with thermochemical data, and checked whether the results

(25) Eliel, E. L.; Wilen, S. H. *Stereochemistry of Organic Compounds*; Wiley: New York, 1994.
(26) (a) Winstein, S.; Holness, N. J. *J. Am. Chem. Soc.* **1955**, *77*, 5562−5578. (b) Eliel, E. L.; Lukach, C. A. *J. Am. Chem. Soc.* **1957**, *79*, 5986−5992.

were compatible with the S_N2-type mechanism postulated before. It is remarkable to note that a simple mechanism and its minor modification can explain all the experimental data adequately, even though not definitively. A major finding in this work is that the conformer-specific dissociation occurs for i-$C_4H_9I^{+\bullet}$ in the excited electronic state, different conformers generating different products in exactly the same fashion as was observed for 1-$C_3H_7I^{+\bullet}$. Also it has been demonstrated in the gas phase that a particular conformation can be a gateway to a particular reaction as has long been postulated in stereochemistry.

JA025791E